Oikos 116: 53–64, 2007
doi: 10.1111/j.2006.0030-1299.14940.x,

Subject Editor: André de Roos, Accepted 28 August 2006

A tale of two cycles – distinguishing quasi-cycles and limit cycles in finite predator–prey populations

Mario Pineda-Krch, Hendrik J. Blok, Ulf Dieckmann and Michael Doebeli

M. Pineda-Krch (pineda@zoology.ubc.ca), H. J. Blok and M. Doebeli, Dept of Zoology and Dept of Mathematics, Univ. of British Columbia, Vancouver, Canada BC V6T 1Z4. Present address for MP-K: Center for Animal Disease Modeling and Surveillance, Dept of Medicine and Epidemiology, School of Veterinary Medicine, Univ. of California, Davis, CA 95616, USA. – U. Dieckmann, Evolution and Ecology Program, Int. Inst. for Applied System Analysis, Schlossplatz 1, AT-2361 Laxenburg, Austria.

Periodic predator–prey dynamics in constant environments are usually taken as indicative of deterministic limit cycles. It is known, however, that demographic stochasticity in finite populations can also give rise to regular population cycles, even when the corresponding deterministic models predict a stable equilibrium. Specifically, such quasi-cycles are expected in stochastic versions of deterministic models exhibiting equilibrium dynamics with weakly damped oscillations. The existence of quasi-cycles substantially expands the scope for natural patterns of periodic population oscillations caused by ecological interactions, thereby complicating the conclusive interpretation of such patterns. Here we show how to distinguish between quasi-cycles and noisy limit cycles based on observing changing population sizes in predator–prey populations. We start by confirming that both types of cycle can occur in the individual-based version of a widely used class of deterministic predator–prey model. We then show that it is feasible and straightforward to accurately distinguish between the two types of cycle through the combined analysis of autocorrelations and marginal distributions of population sizes. Finally, by confronting these results with real ecological time series, we demonstrate that by using our methods even short and imperfect time series allow quasi-cycles and limit cycles to be distinguished reliably.

Many natural populations exhibit cyclic fluctuations. Some well-known examples include numerous species of mammals in the boreal zone of Eurasia and North America (Elton 1942, Turchin and Ellner 2000, Gilg et al. 2003), cyclic outbreaks of feral house mice in Australia (Korpimäki et al. 2004), Dungeness crab cycles in the Pacific North America (Higgins et al. 1997), and forest insect cycles (Liebhold and Kamata 2000).

Explaining the underlying mechanisms of population cycles is a central problem in ecology and has preoccupied population ecologists ever since Elton's classical work (Elton 1924, Krebs 1985, Lindström et al. 2001, Berryman 2002, Korpimäki et al. 2004). Two different mechanisms are chief among the many hypotheses proposed to date for the origin of population cycles: it is widely acknowledged that such cycles can be generated either by extrinsic environmental mechanisms, such as periodic environmental regimes (Grover et al. 2000, Korpimäki et al. 2004) or random environmental perturbations (Nisbet and Gurney 1976), or by intrinsic ecological interactions, such as competition and predation, that give rise to intrinsic cyclic dynamics described by limit cycles (May 1974, Gilg et al. 2003).

Over the years, a multitude of models have been formulated and explored with the goal of determining conditions that enhance or inhibit population cycles. Most of these models rely on the assumption that populations sizes are infinite, and hence implicitly on the assumption that the effects of demographic stochasticity are negligible for predator–prey dynamics. It is known, however, that demographic stochasticity arising from random birth and death events in finite populations can generate persistent large-amplitude cycles if the corresponding deterministic model converges to its equilibrium through weakly damped oscillations (Bartlett 1957, Renshaw 1991, Gurney and Nisbet

1998, McKane and Newman 2005). The mechanism generating such quasi-cycles is distinct from other proposed causes generating cyclic dynamics. Because quasi-cycles are expected to arise whenever a continuous system exhibits a stable focus, which can already occur in linear systems, they offer a simpler alternative to stable limit cycles, which always require non-linear population models. The existence of quasi-cycles complicates, however, the interpretation of cycles observed in finite populations, in particular when the underlying ecological interactions can exhibit stable foci as well as stable limit cycles, as is the case in the models presented here.

The pattern of fluctuations in a population is intimately linked to the deterministic properties of the studied system. Consequently, differentiating between quasi-cycles and noisy limit cycles is important for identifying causal relationships and understanding how ecological interactions regulate predator–prey populations, as the structural prerequisites (e.g. in terms of ecological mechanisms) for the two types of cycle tend to differ. It is not clear, however, how such a distinction can be achieved in practice, based on fluctuating and inherently noisy time series. We address this question by first demonstrating the existence of quasi-cycles in a stochastic birth–death process derived from deterministic models that exhibit both stable equilibria and stable limit cycles. By analyzing noisy time series of simulated predator-prey dynamics using a combination of two types of analysis we show that it is feasible to accurately distinguish between quasi-cycles and noisy limit cycles, even when using data from only one of the species. Finally, by applying the methods of analysis developed here to a number of real time series of population sizes, we show that our approach gives consistent and useful results for ecological data observed in nature.

Model

The model used here for illustration is based on Lotka–Volterra predator–prey dynamics with density-dependent growth in the prey and a nonlinear type-2 functional response in the predator (also referred to as the Rosenzweig-MacArthur predator–prey model, Rosenzweig and MacArthur 1963, Kot 2001). In the absence of demographic stochasticity, this model is deterministic and given by the following equations,

$$\frac{dN}{dt} = (b-d)N\left(1-\frac{N}{K}\right) - \frac{aN}{1+wN}P,$$
$$\frac{dP}{dt} = P\left(c\frac{aN}{1+wN} - g\right). \quad (1)$$

Here N and P are the densities of prey and predator, respectively, b and d are the intrinsic per capita birth and death rates of the prey (so that b–d is the prey's intrinsic per capita growth rate), K is the carrying capacity of the prey, a is the predation efficiency, c is the conversion efficiency of the predator (given by the average number of predator offspring produced per consumed prey) and g is the per capita death rate of the predator. The parameter w measures the degree of predator saturation. When $w>0$, the rate of prey consumption by the predator gradually increases as prey density increases, exhibiting a diminishing return before eventually leveling off at a/w. The limit $w=0$ corresponds to a linear functional response, allowing the consumption rate to increase indefinitely in proportion with prey density. All other parameters are assumed to be positive.

It is well known that this model can possess three equilibria (N^*, P^*) one at which both species are extinct, ($N^*=0$, $P^*=0$); one at which the predator is extinct while the prey is at its carrying capacity, ($N^*=K$, $P^*=0$); and one at which the two species coexist, $(N^* = \frac{g}{ca-gw},\quad P^* = \frac{c(b-d)(K(ca-gw)-g)}{K(ca-gw)^2})$ (Hastings 1998). Reasonable biological assumptions ensure that the first two equilibria are always unstable, while the coexistence equilibrium may or may not be locally stable (Kot 2001 for details). If the coexistence equilibrium is locally stable, it can be approached in one of two ways. Either the equilibrium is a stable node, so that the approach to the equilibrium occurs without oscillations, or the equilibrium is a stable focus, so that the approach occurs through damped oscillations. If the coexistence equilibrium is locally unstable, it can be an unstable node, a saddle point or an unstable focus. If, in the latter case, the functional response is nonlinear ($w>0$), the trajectory converges to a closed orbit around the unstable focus, giving rise to a stable limit cycle. Fig. 1 shows parameter regions of the model resulting in any of the three alternative attractors enabling the coexistence of prey and predator: stable node, stable focus and stable limit cycle. The frequency of oscillations around the stable foci and along the stable limit cycles can be determined analytically (Bulmer 1994, Hastings 1998, Kot 2001).

To incorporate the effects of demographic stochasticity on the population dynamics in finite predator and prey populations, we formulated an individual-based version of the deterministic model in Eq. 1 as a stochastic birth-death process. In the stochastic model, birth and death events occur at probabilistic rates derived from the deterministic Eq. 1. Thus, birth events in the prey population occur at a rate $B_N = bN$, while prey death occurs at a rate $D_N = dN + \frac{b-d}{K}N^2 + \frac{a}{1+wN}NP$. Here N and P are not densities, but the actual (finite) numbers

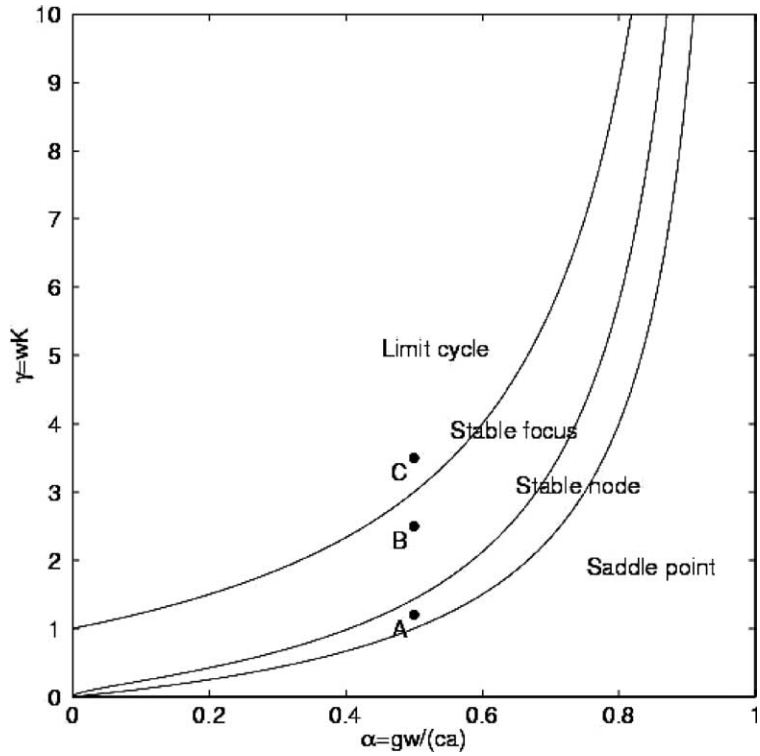

Fig. 1. Alternative coexistence regimes of the studied predator-prey dynamics. Points A, B and C highlight parameter combinations situated in each of the three possible coexistence regimes: stable node (A), stable focus (B) and stable limit cycle (C). Note that in the parameter region labeled "Saddle point" the predator and prey populations cannot stably coexist. Parameters: $\alpha = 0.5$ (ABC), $\gamma = 1.2$ (A), $\gamma = 2.5$ (B), $\gamma = 3.5$ (C).

of prey and predator individuals at any given point in time. Similarly, predator birth occurs at rate $B_p = c\frac{a}{1 + wN}NP$, and predator death at rate $D_P = gP$.

The dynamics of the stochastic model unfolds as follows. At any given point in time, with current population size N and P, the birth and death rates are calculated as above, and the next event occurring is chosen randomly according to the four probabilities $\frac{B_N}{E}$, $\frac{D_N}{E}$, $\frac{B_P}{E}$, and $\frac{D_P}{E}$, where $E = B_N + D_N + B_P + D_P$ is the total event rate. If the chosen event is a prey birth, N is increased by 1, if it is a prey death, N is decreased by 1, with analogous actions for the predator birth and death events. After an event has occurred, all birth and death rates are calculated anew, and the next event is chosen based on the new rates. It is assumed that the time lapse between two successive events is drawn from an exponential distribution with mean 1/E, where E is the total current event rate. Thus, when E is high, little time passes between events, whereas time lapses become long when E is low.

To explore the behavior of the stochastic model we ran a large number of simulations throughout parameter space, concentrating attention on parameter combinations for which the predator–prey dynamics are predicted to converge to a stable node, a stable focus, or a stable limit cycle. Specific parameter combinations for which results are presented are indicated in Fig. 1. Unless otherwise stated, all simulations were started at equilibrium population sizes and run for 10 000 time units. Population sizes were censused in intervals of 1 time unit.

Results

Analysis of simulated time series

Extensive numerical simulations showed that when the underlying deterministic system had a stable focus, demographic stochasticity consistently gave rise to persistent and periodic large-amplitude population cycles (Fig. 2B). Since these so-called quasi-cycles arise in parameter regions in which infinite populations would instead converge to a stable equilibrium, they are critically driven by the demographic stochasticity

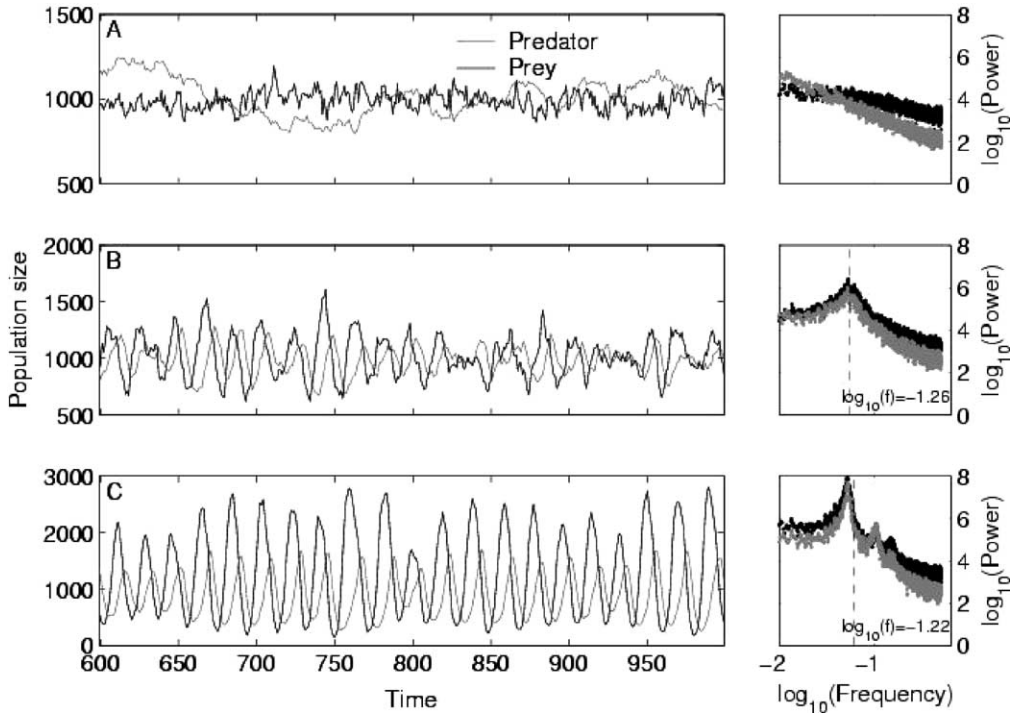

Fig. 2. Time series (left column) and power spectra (right column) resulting from simulated predator–prey dynamics in finite populations. Prey-related quantities are depicted in black and predator-related quantities in gray. Panels show results for each of the three alternative coexistence regimes: stable node (A), stable focus (B) and stable limit cycle (C), with parameters chosen as in Fig. 1. To aid the interpretation of time, note that the unit of time equals the average lifespan of the prey, 1/d, in the absence of predation (d = 1 in all simulations). All power spectra are based on the full simulated time series (10 000 time units) and were estimated through fast Fourier transform.

resulting from the random birth and death events in finite populations. Simulations throughout the parameter region in which the deterministic model exhibits a stable focus demonstrated the ubiquity of quasi-cycles in this region (results not shown), thus confirming many analogous earlier observations and predictions (Bartlett 1957, Nisbet and Gurney 1976, Renshaw 1991, Gurney and Nisbet 1998, McKane and Newman 2005). Quasi-cycles, in general, are expected whenever the convergence toward a stable focus is perturbed by noise.

As anticipated, the stochastic model simply results in a noisy limit cycle throughout the parameter region in which the underlying deterministic model converges to a stable limit cycle (Fig. 2C). Finally, in parameter regions in which the deterministic model exhibited a stable node, the stochastic model exhibited fluctuations without any distinctive oscillatory pattern (Fig. 2A). The presence and absence of periodic and persistent population cycles in the focus and limit cycle regime was confirmed by spectral analysis (right column in Fig. 2).

To investigate how best to distinguish between quasi-cycles and noisy limit cycles, below we introduce two methods of time series analysis and apply them to the simulated predator–prey dynamics described above. These two methods are based, respectively, on evaluating the shapes of autocorrelation functions and marginal distributions.

Autocorrelation functions

A common technique for analyzing time series is to estimate their autocorrelation function (ACF). Autocorrelations measure the correlation, throughout a time series, between fluctuations at varying time lags (Gurney and Nisbet 1998). In general, ACFs are used to determine the characteristic time scale at which a dynamical system ''forgets'' its state through the impact of random fluctuations. In particular, if a system exhibits population cycles, the ACF inherits the periodicity at the cycle's frequency.

The ACF of the simulated predator–prey time series showed clear periodicity in the case of quasi-cycles and noisy limit cycles (Fig. 3B–C), while such periodicity was absent in the case of noisy nodes (Fig. 3A). Although both quasi-cycles and noisy limit cycles

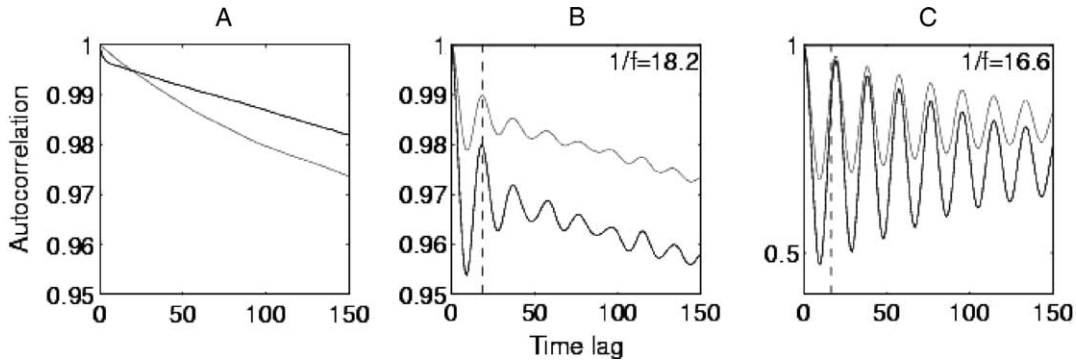

Fig. 3. Autocorrelation functions resulting from simulated predator–prey dynamics in finite populations. Prey-related quantities are depicted in black and predator-related quantities in gray. Panels show results for each of the three alternative coexistence regimes: stable node (A), stable focus (B) and stable limit cycle (C), with parameters chosen as in Fig. 1. Note the different scale for the vertical axis in (C). Dashed lines in (B) and (C) indicate the predicted cycle period, with values indicated in the top right corner of these plots. The autocorrelation functions are normalized so as to assume ordinate 1 at time lag 0.

yielded a periodic ACF, there were important qualitative differences between the ACF signatures of these two types of oscillation. For quasi-cycles, the ACF showed low-amplitude oscillations and a rapid loss of phase information, resulting in the strong damping of ACF oscillations within the first few periods (Fig. 3B). For the noisy limit cycles, the ACF oscillations were much more pronounced and were maintained at high amplitude for many cycles, indicating the longer (i.e. more accurate) phase memory that the system exhibits in this dynamical regime (Fig. 3C). Comparing the rate of decay in the oscillations of the ACF from a large number of time series exhibiting quasi-cycles and noisy limit cycles consistently showed that for quasi-cycles a virtually complete loss of periodicity in the autocorrelation occurred within just a few cycle periods.

The decay rate of oscillations in the ACF can be estimated by quantifying the width of the envelope of ACF oscillations at a time lag of one cycle period. The upper and lower bounds of this envelope are defined, respectively, by the local peaks and troughs of a periodic ACF. Since we are interested in the relative decay of oscillations in the ACF, rather than in the absolute magnitude of the autocorrelations, these upper and lower bounds are determined from the normalized ACF, for which the autocorrelation at time lag 0 is scaled to 1 (Nisbet and Gurney 1982). The ordinate of the second peak in the ACF (which follows the first peak at lag 0 and ordinate 1) provides an estimate of the envelope's upper bound at a time lag of one cycle period. Likewise, a linear interpolation between the ACF's first two troughs provides an estimate of the envelope's lower bound, again at a time lag of one cycle period. We can thus approximate the lower bound of the envelope of ACF oscillations at a time lag of one cycle period by the arithmetic mean of ordinates at the ACF's first two troughs. An estimate of the amplitude of ACF oscillations at a lag of one cycle period is then given by halving the difference between the oscillation envelope's upper and lower bounds at this time lag.

Using this method to analyze the simulation results clearly shows that, for both the prey and the predator, the amplitude of ACF oscillations after one cycle period remains above 0.05 in the case of noisy limit cycles, whereas this amplitude falls well below 0.05 in the case of quasi-cycles (Fig. 3). This defines a heuristic threshold that can be used to as a criterion for distinguishing between the rapidly and slowly decaying oscillations in ACFs resulting, respectively, from quasi-cycles and limit cycles.

Marginal distributions

Multivariate time series can be assessed by analyzing the marginal distributions resulting for each of the time series' components. The joint distribution of predator and prey population sizes is given by a two-dimensional histogram, indicating the frequencies with which different combinations of prey and predator population sizes occur (top row in Fig. 4). The corresponding marginal distributions of prey population size (shown) or predator population size (not shown) are given by one-dimensional histograms (bottom row in Fig. 4).

It can be shown analytically that, for sufficiently low levels of noise, the joint distribution of predator and prey population sizes in a stochastic model whose underlying deterministic dynamics has a stable equilibrium is bivariate normal (Appendix V in May 1974, van Kampen 1981). The mean, N, of this distribution is close to the equilibrium population sizes predicted from the deterministic model, and the standard deviation in each component is proportional to $\sqrt{N}$ (May 1974, McKane and Newman 2005). Hence, fluctua-

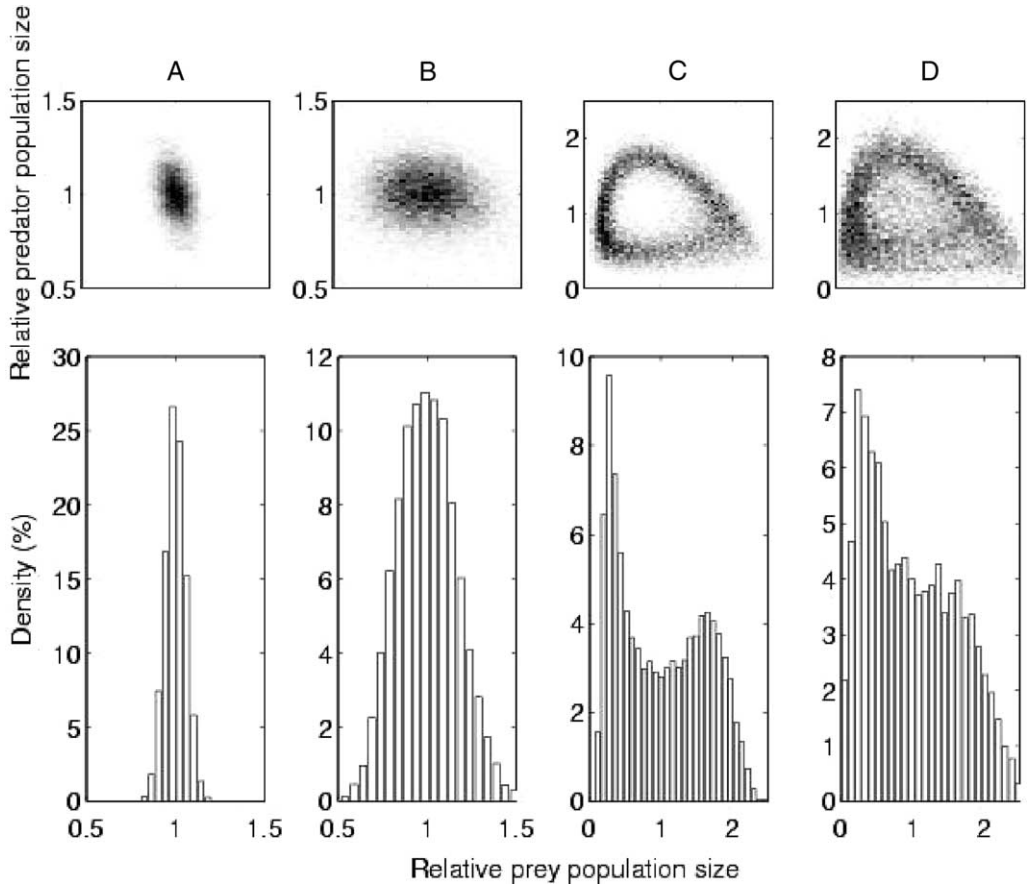

Fig. 4. Joint distributions of predator and prey population sizes (top row) and marginal distributions of prey population sizes (bottom row) resulting from simulated predator–prey dynamics in finite populations. Columns show results for each of the three alternative coexistence regimes: stable node (A), stable focus (B) and stable limit cycle regime (C and D), with parameters chosen as in Fig. 1. Other parameters: $N^* = P^* = 1000$ (ABC), $N^* = P^* = 300$ (D).

tions measured relative to the population mean typically decrease as $1/\sqrt{N}$ as the mean population grows. This general result implies that the marginal distributions of population size in each species are normal.

Likewise, it can be shown analytically that, for sufficiently low levels of noise, the joint distribution of predator and prey population sizes in a stochastic model whose underlying deterministic dynamics has a stable limit cycle takes the shape of a crater ridge (Olarrea and de la Rubia 1996). This general result implies that the marginal distributions of population sizes in each species are non-normal, and possibly bimodal. By contrast, for very high levels of noise, the joint distribution of predator and prey population sizes along a noisy limit cycle becomes bivariate normal, and, accordingly, also the marginal distributions of population size in each species become normal.

Extensive simulations of our stochastic predator-prey model confirm these predictions. For parameter combinations exhibiting noisy nodes and quasi-cycles, both the joint distribution and the marginal distributions were normal (Fig. 4A–B). In contrast, parameter combinations resulting in noisy limit cycles confirmed the prediction of a crater ridge in the joint distribution, resulting in non-normal marginal distributions (Fig. 4C). Even with population sizes were as low as $N^* = P^* = 300$ (Fig. 4D), implying very high levels of demographic stochasticity, the crater ridge was easily detected.

These observations suggest that joint and marginal distributions may be used to distinguish noisy limit cycles from either quasi-cycles or noisy nodes. In particular, the observation of significant non-normality in joint and marginal distributions is indicative of underlying limit cycles, and sufficient for rejecting a hypothesis of quasi-cycles. To evaluate the practical feasibility of this approach, we tested a large number of simulated time series for normality. For this purpose we

applied two test statistics: the Kolmogorov–Smirnov test (KS) and the D'Agostino–Pearson K^2 test (K^2).

Using the Kolmogorov–Smirnov (KS) test with the Dallal–Wilkinson–Lilliefors correction (Lilliefors 1967, Dallal and Wilkinson 1986) and the D'Agostino–Pearson K^2 test (D'Agostino et al. 1990), the simulated and real ecological time series were assessed for normality. Although the K^2 test of normality is considered superior to the KS test, the latter is the more common of the two (D'Agostino et al. 1990). Here we included both test statistics as examples of a strong but rarely used statistic (K^2) and a weak but common statistic (KS). The KS tests were performed using the lillietest function in MatLab (Statistics Toolbox version 3.0) and the K^2 tests were performed using the DagosPtest function in MatLab (Trujillo-Ortiz and Hernandez-Walls 2003). For both statistics, we assumed a confidence level of $P < 0.05$ and the null hypothesis that samples were drawn from a normal distribution. To perform the normality tests on more realistic data sizes and to evaluate the consistency of the test results, each full time series (10 000 time units long) was split into segments of 100 time units. To remove the effects of transients, the first nine segments were discarded and the tests were performed on the remaining 91 segments.

When applied to our stochastic predator–prey model, the results of the normality tests (Table 1) were consistent with the predictions summarized above. While a majority of noisy nodes and quasi-cycles gave rise to marginal distributions that were significantly normal (75% of the noisy nodes and 91% of the quasi-cycles), the hypothesis of normality could be rejected, at a confidence level of , for all data originating from noisy limit cycles (Table 1). The reason why the marginal distributions for some of the noisy nodes and quasi-cycles did not conform to normality is due to the magnitude of demographic noise (May 1974). Further simulations confirmed that, as the level of demographic stochasticity decreases for larger populations, the proportion of marginal distributions correctly identified as being normal increases (results not shown).

Although the results in Table 1 suggest that tests of normality in the prey's time series are more accurate than in the predator's time series (93% correctly identified as normal in the prey vs 72% in the predator), the mechanistic basis for this pattern has to be determined before it can be generalized outside the context of the present model. As expected, the K^2test, widely acknowledged as being stronger than the KS test, turns out to be more accurate in identifying normality (90% correctly identified as normal in the K^2 test vs 75% in the KS test).

Analysis of real ecological time series

To evaluate the usefulness of combining the analysis of autocorrelation functions and marginal distributions for distinguishing between quasi-cycles and noisy limit cycles, we applied both approaches to three different time series of naturally observed population sizes.

The time series we analyzed were Hudson Bay Company fur count records of lynx-hare, otter and wolverine. Ever since Elton's (1924) groundbreaking work on the population dynamics of boreal mammals, fur counts such as trapping and sales records have been widely used as indirect estimates of relative population densities. Among the ecological time series analyzed here, the hare, otter, and wolverine data sets consists of fur sales records while the lynx time series consists of a combination of trapping and sales records. Here we will refer to both types of records as fur counts or simply counts. Results of these analyses are summarized in Table 2.

Lynx–hare time series

The classical Hudson Bay Company lynx–hare time series consists of fur counts from different regions of Canada and has, over the years, been extensively studied. The current interpretation of the lynx–hare cycles is that limit-cycle dynamics are generating the population cycles (Krebs et al. 2001). Nisbet and Gurney (1976), however, interpret the lynx oscillations in terms of quasi-cycles. Earlier work (Moran 1953) had already established that the lynx–hare cycles are

Table 1. Statistical tests of normality of the marginal distributions of population sizes using the Kolmogorov–Smirnov test and the D'Agostino–Pearson K^2 test (see main text for details). The null hypothesis is that the sample of population sizes originates from a normal distribution. The percentages given in the table indicate the fraction of marginal distributions for which normality was significant, out of 91 analyzed time series. $N^* = P^* = 20{,}000$ for the node and focus, and $N^* = P^* = 10{,}000$ for the limit cycle.

Deterministic behavior	Stochastic behavior	KS		K^2	
		Predator	Prey	Predator	Prey
Node	noisy node	36%	93%	73%	96%
Focus	quasi-cycle	84%	87%	96%	97%
Limit cycle	noisy limit cycle	0%	0%	0%	0%

Table 2. Analysis of simulated and real time series of population sizes. The table's section on simulated time series summarizes the predictions for three alternative coexistence regimes, based on the results presented in Figs. 3 and 4. The section on real time series summarizes the analyses presented in Fig. 5–7. The density distributions were analyzed for normality using the Kolmogorov–Smirnov test and the D'Agostino-Pearson test (see main text for details).

Time series		Oscillations in ACF	Marginal distribution		Stochastic behavior
			KS	K^2	
Simulated	node	none	normal	noisy node	
	focus	rapidly decaying	normal	quasi-cycle	
	limit cycle	slowly decaying	non-normal	noisy limit cycle	
Real	lynx-hare	slowly decaying	non-n.	non-n.	noisy limit cycle
	otter	none	normal	normal	noisy node
	wolverine	rapidly decaying	normal	normal	quasi-cycle

likely caused by intrinsic ecological interactions, as opposed to mere environmental forcing.

The time series we analyzed are obtained from Elton and Nicholson (1942) and consist of the total count from all the trapping regions. The lynx time series (Fig. 5A) consists of fur counts from the years 1736–1907 spanning 173 years (with no missing years) and the hare time series (Fig. 5A) consists of counts from the years 1788–1936 spanning 149 years (with several blocks of missing years). The autocorrelation functions (Fig. 5B) exhibit clear and persistent oscillations with a cycle period of approximately 10 years, which is maintained for well over five cycle periods (the amplitude of oscillation in the normalized autocorrelation at a time lag of one cycle period is above 0.05). The marginal distributions (Fig. 5C–D) are strongly skewed toward high values with the majority of counts having low values, which is reflected by the rejection of normality by both test statistics (Table 2). Hence, the results from both the autocorrelation functions and the marginal distributions are consistent with interpreting the observed oscillations in terms of a noisy limit cycle

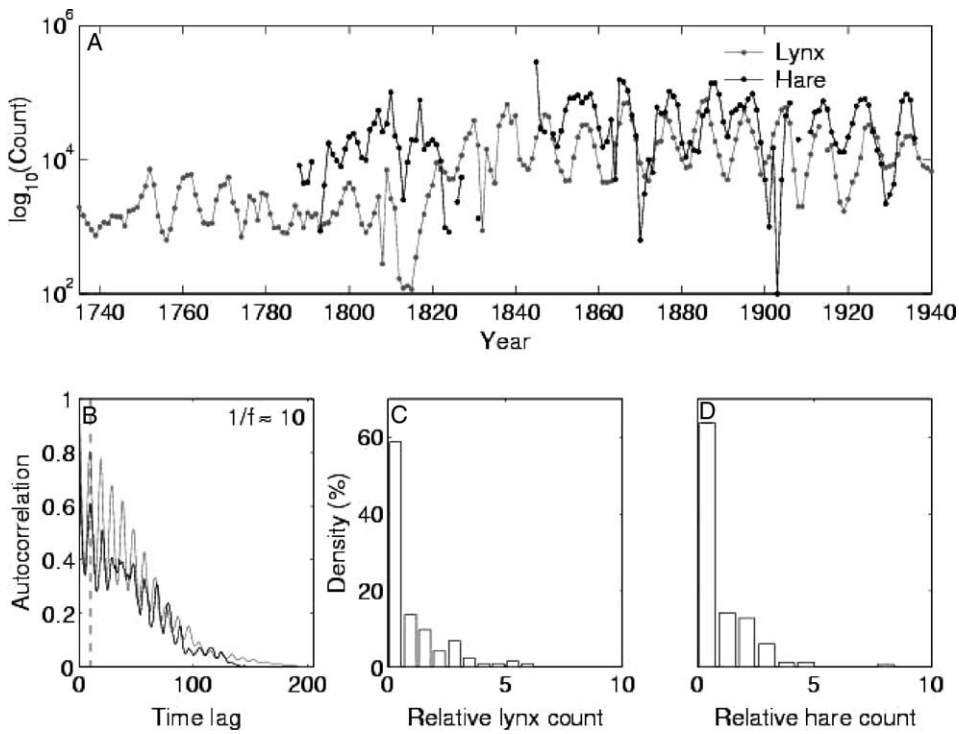

Fig. 5. Analysis of the lynx–hare time series. (A) Time series (note $\log_{10}$ scale on vertical axis), (B) autocorrelation functions of lynx and hare, (C) marginal distribution of lynx abundances relative to their mean, and (D) marginal distribution of hare abundances relative to their mean. The dashed line in (B) indicates the approximate period of the population cycles, $1/f \approx 10$ years.

which is in contrast to Nisbet and Gurney's (1976) interpretation.

Otter time series

The otter time series was obtained from the Time Series Data Library (Hyndman 2005) and spans 62 years of fur counts between the years 1850–1911 (Fig. 6A). The autocorrelation function is non-periodic and linearly decaying, a result that is consistent only with interpreting the observed fluctuations in terms of a noisy node (Fig. 6B). This conclusion is supported by both test statistics identifying the distribution of abundances (Fig. 6C) as significantly normal (Table 2).

Wolverine time series

The time series of wolverine abundances was obtained from the Time Series Data Library (Hyndman 2005) and spans 62 years (Fig. 7A). The autocorrelation function possesses a weak and rapidly decaying oscillations (Fig. 7B). In particular, the amplitude of oscillations in the normalized autocorrelation function at a time lag of one cycle period is below 0.05, which is consistent with interpreting the observed oscillations in terms of quasi-cycles. This conclusion is supported by both test statistics identifying the distribution of abundances (Fig. 7C) as significantly normal (Table 2).

Discussion

In this study we have tried to elucidate how to distinguish between quasi-cycles and limit cycles in finite predator–prey populations. We addressed this question by first investigating a stochastic birth–death model that, based on an analysis of the underlying deterministic predator–prey model, was predicted to exhibit both types of cycles. A large number of stochastic simulations confirmed this prediction. We then considered which methods of time series analysis would be most helpful for identifying the deterministic dynamics underlying observed population cycles. Two particular methods, based on autocorrelation functions and marginal distributions, were singled out for closer investigation. Application of these methods to data obtained from our stochastic predator–prey model, as well as from a number of real ecological time series, demonstrated their ability to differentiate between the two alternative origins of population cycles generated by ecological interactions.

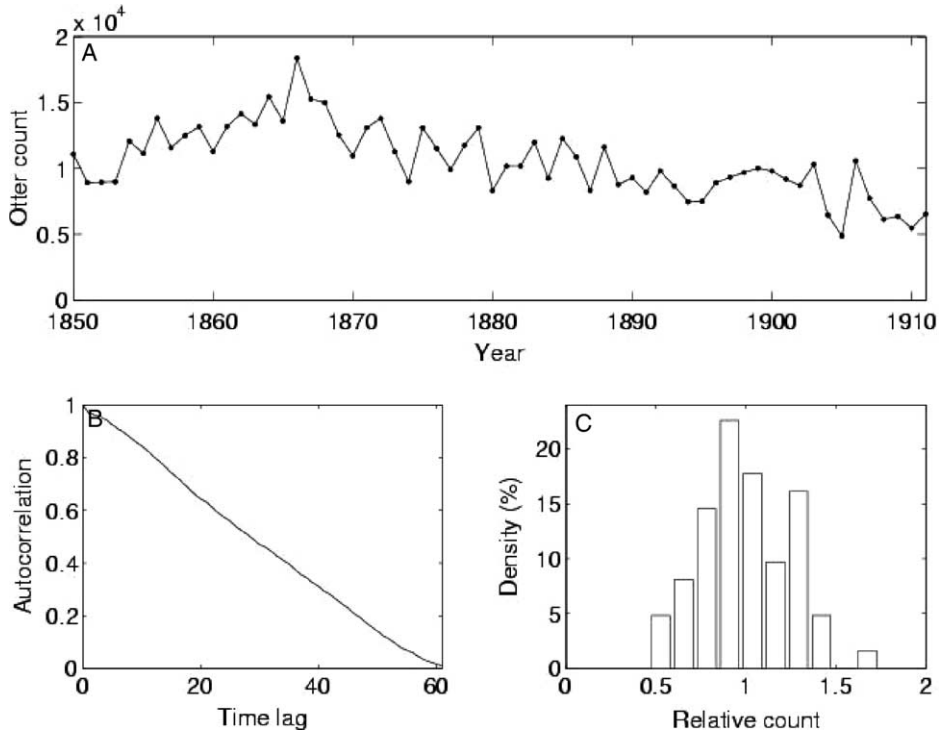

Fig. 6. Analysis of the otter time series. (A) Time series, (B) autocorrelation function, (C) distribution of relative abundances.

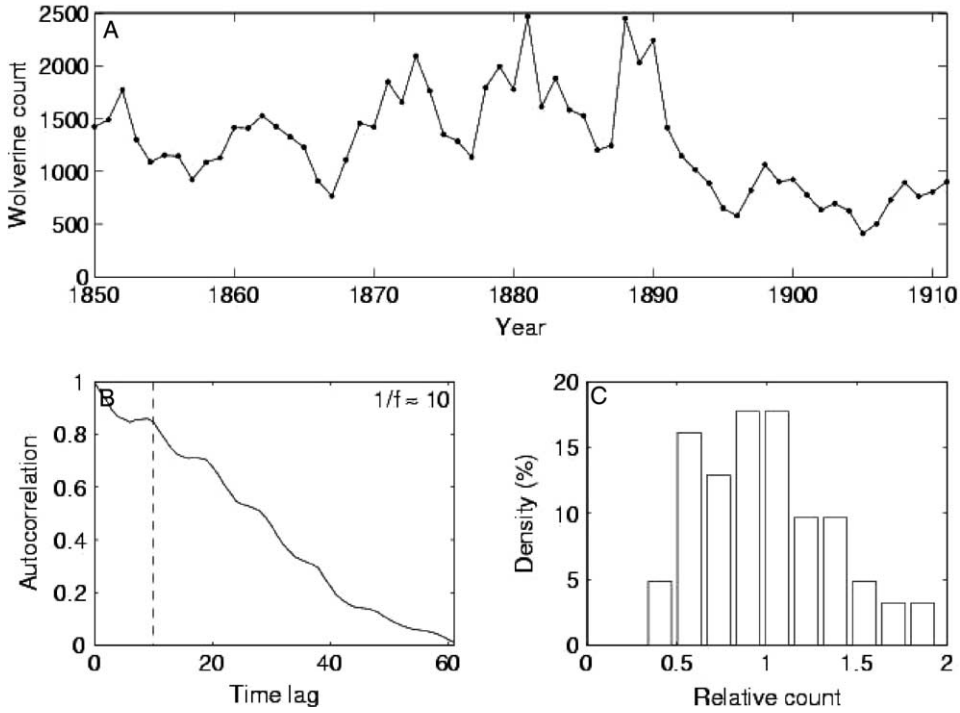

Fig. 7. Analysis of the wolverine time series. (A) Time series, (B) autocorrelation function, and (C) distribution of relative abundances. The dashed line in (B) indicates the approximate period of the population cycles, $1/f \approx 10$ years.

The existence of quasi-cycles has previously been demonstrated in models exhibiting stable equilibria (Bartlett 1957, Nisbet and Gurney 1976, Renshaw 1991, Gurney and Nisbet 1998, McKane and Newman 2005). These studies predicted that the existence of quasi-cycles should generalize to any deterministic model that exhibits a stable focus and is perturbed by noise. Our study confirms these earlier predictions and extends the previous analyses in two ways. First, we generalized preceding theoretical studies to a larger class of models that deterministically can exhibit both stable foci and stable limit cycles. This extension provided us with a unified platform for investigating how, in a constant environment, periodic and persistent cycles in finite predator–prey populations can arise from two alternative mechanisms, when the deterministic skeleton of the considered stochastic process predicts either a stable limit cycle or a stable equilibrium approached through damped oscillations. Second, we addressed the obvious question of how one can distinguish between these two types of cycles. Here we have shown how two complementary methods of time series analysis can help to accurately identify the appropriate deterministic skeleton of a noisy time series showing population cycles, even when in a two-species dynamics only one of the time series is observed.

Our recommended analysis of noisy predator–prey time series consists of two complementary methods, based in turn on the autocorrelation function (ACF) and the statistical analysis of the normality of the marginal distribution, each carried out on the time series from one of the species at a time. Out of these two techniques, analysis of the ACF showed the most promise as a first method of choice. The advantage of this method is that it is capable of distinguishing between all three types of stochastic behavior: noisy nodes, quasi-cycles and noisy limit cycles. In contrast, analysis of the normality of the marginal distribution is primarily useful for accurately distinguishing quasi-cycles and noisy nodes from noisy limit cycles. This makes marginal distributions a recommendable secondary target of analysis, particularly if the interpretation of the ACF is inconclusive.

The first step in interpreting the ACF is to assess it for periodicity. While a periodic ACF is consistent with population cycles (which could either be quasi-cycles or noisy limit cycles), a non-periodic ACF is only consistent with a noisy node (Fig. 3A). The ACF of the otter time series reveals such a non-periodic sequence (Fig. 6B). If the ACF is periodic, the next step is to assess the amplitude of the ACF's oscillations and the rate at which these decay with increasing time lag. It is difficult to quantify the distinction between rapidly and slowly decaying ACF without exploring more than a single model. As a general rule of thumb, however, the hallmark of rapidly decaying oscillations is

loss of periodicity within a few cycle periods (Fig. 3B), while slowly decaying oscillations maintain a high-amplitude periodic component for many cycle periods (Fig. 3C). Our results show that slowly decaying oscillations can be identified by an oscillation amplitude in the normalized ACF that exceeds 0.05 after one cycle period, whereas rapidly decaying oscillations exhibit a substantially faster decay of that oscillation amplitude. Applying this criterion to the ecological time series clearly identifies the oscillations in the lynx–hare ACF as slowly decaying (Fig. 5B, Table 2), and as rapidly decaying in the wolverine ACF (Fig. 7B, Table 2).

The analysis of the marginal distributions can be used to confirm the results obtained from the ACF. More importantly, however, investigating the normality of marginal distributions offers an alternative approach when an assessment of the ACF is inconclusive. For example, if the decay rate of a periodic ACF is unclear, analysis of the marginal distribution can help to decide whether observed population cycles are due to quasi-cycles or limit cycles. If it is difficult to determine if there is a periodic component in the ACF in the first place, analysis of the marginal distribution can only accurately distinguish between a noisy limit cycle on the one hand (when normality is rejected) and a quasi-cycle or noisy node on the other (when normality is accepted). When applying the combined analysis of autocorrelation functions and marginal distributions to the three ecological time series investigated in this study, results from the two alternative normality test statistics were always consistent with each other and with the conclusions drawn from the ACF. The observed consistency may bode well for the conclusiveness of this type of analysis when applied to other time series.

A third diagnostic tool that can be useful when analyzing noisy time series is the power spectrum (Platt and Denman 1975). Power spectra reveal the frequency content of the time series and can detect the presence of periodic population cycles, easily identified by a peak in the spectrum. A limitation of power spectra, and the reason this method is not part of our recommended set of analyses here, is that power spectra cannot distinguish between quasi-cycles and noisy limit cycles (compare Fig. 2B with 2C). A second, practical limitation, which is especially important when analyzing real ecological data, is that power spectra require substantially longer time series (i.e. more data points) to detect regular cycles than the ACF. Our numerical analysis of power spectra indicated that a minimum of 25 cycle periods is required for a power spectrum to detect oscillations reliably (results not shown). The vast majority of ecological time series are therefore far too short for power spectra to accurately detect population cycles.

An important assumption when interpreting population cycles in terms of either quasi-cycles or limit cycles is that the populations' environment is constant. Without additional information, it is not possible to eliminate the possibility that population fluctuations identified as quasi-cycles or noisy limit cycles are actually driven by periodic environmental regimes. For example, even though our analyses identified the lynx–hare fluctuations as noisy limit cycles, which supports the current consensus (Krebs et al. 2001), possible effects of periodic external variables cannot be ruled out. It has been suggested, for example, that the intrinsic lynx–hare cycles are intermittently synchronized by climate cycles (Sinclair et al. 1993, Krebs et al. 2001). The effects of episodic or continuous external periodic forcing on limit cycles and quasi-cycles are currently not sufficiently well known. One could speculate, for example, whether dynamics akin to limit cycles (identified as such by the ACF and the marginal distribution) could result from quasi-cycles modulate by an external periodic variable.

In the real world, the environment is never constant. Even in the absence of periodic environmental regimes, real populations always experience random perturbations due to the inherent uncertainty of environments. While the quasi-cycles that we have analyzed here are entirely driven by demographic stochasticity, it is well known that random environmental perturbations also can generate quasi-cycles (Nisbet and Gurney 1976). We thus expect that our recommended analysis is equally suitable for distinguishing limit cycles from quasi-cycles generated by random environmental perturbations.

The possibility for endogenous quasi-cycles considerably expands the scope for population fluctuations caused by intrinsic ecological interactions, since quasi-cycles can be expected whenever the underlying deterministic population model exhibits damped oscillations toward an equilibrium. To explain the causal basis of population cycles, it then becomes important to be able to distinguish quasi-cycles from limit cycles. Our results are promising in that they suggest that systematically applying a set of simple analyses to data from natural populations can accurately distinguish between quasi-cycles and limit cycles.

Acknowledgements – We thank the Dept of Zoology ''Dirt Lunch'' participants, André de Roos, and Bill Gurney for constructive feedback. The simulations were performed on the PIII/Linux cluster at the Dept of Physics and the Beowulf cluster at the Inst. of Applied Mathematics of the Univ. of British Columbia. We are grateful to Rob J. Hyndman (Time Series Data Library) for the permission to use the otter and wolverine time series. This research was supported by the James S. McDonnell Foundation (USA), by NSERC (Canada) and by the Pacific Inst. for the Mathematical

Sciences (Canada). UD is indebted to Jonathan Dushof for pointing out the early consideration of quasi-cycles in the epidemiological research of the late Maurice S. Bartlett, and to Richard Law for originally attracting his attention to the phenomenon of quasi-cycles in individual-based models.

References

Bartlett, M. S. 1957. Measles periodicity and community size. – J. R. Stat. Soc. A 120: 48–70.

Berryman, A.. 2002. Population cycles: cause and analysis. – In: Berryman, A. A. (ed.), Population cycles: the case for trophic interactions. Oxford Univ. Press, pp. 13–28.

Bulmer, M. G. 1994. Theoretical evolutionary ecology., Sinauer Ass. Publishers.

D'Agostino, R. B., Belanger, A. and D'Agostino Jr., R. B. 1990. A suggestion for using powerful and informative test of normality. – Am. Stat. 44: 316–321.

Dallal, G. E. and Wilkinson, L. 1986. An analytical approximation to the distribution of Lilliefors's test statistic for normality. – Am. Stat. 40: 294–296.

Elton, C. 1924. Periodic fluctuations in the numbers of animals: their cause and effects. – Brit. J. Exp. Biol. 2: 119–163.

Elton, C. 1942. Voles, mice and lemmings: problems in population dynamics. – Claredon Press.

Elton, C. and Nicholson, M. 1942. The ten-year cycle in numbers of the lynx in Canada. – J. Anim. Ecol. 11: 215–244.

Gilg, O., Hanski, I. and Sittler, B. 2003. Cyclic dynamics in a simple vertebrate predator–prey community. – Science 302: 866–868.

Grover, J. P., McKee, D., Young, S. et al. 2000. Periodic dynamics in *Daphnia* populations: biological interactions and external forcing. – Ecology 81: 2781–2798.

Gurney, W. C. S. and Nisbet, R. M. 1998. Ecological dynamics. – Oxford Univ. Press.

Hastings, A. 1998. Population biology: concepts and models. – Springer.

Higgins, K., Hastings, A., Sarvela, J. N. et al. 1997. Stochastic dynamics and deterministic skeletons: population behavior of Dungeness crab. – Science 276: 1431–1435.

Hyndman, R. J. 2005. Time Series Data Library. – [WWW document]. URL: http://www-personal.buseco.monash.edu.au/ ~hyndman/TSDL/.

Kot, M. 2001. Elements of mathematical ecology. – Cambridge Univ. Press.

Korpimäki, E., Brown, P. R., Jacob, J. et al. 2004. The puzzle of population cycles and outbreaks of small mammals solved? – BioScience 54: 1071–1079.

Krebs, C. J. 1985. Ecology. The experimental analysis of distribution and abundance. – Harper and Row.

Krebs, C. J., Boonstra, R., Boutin, S. et al. 2001. What drives the 10-year cycle of snowshoe hares? – BioScience 51: 25–35.

Liebhold, A. and Kamata, N. 2000. Are population cycles and spatial synchrony a universal characteristic of forest insect populations? – Popul. Ecol. 42: 205–209.

Lilliefors, H. W. 1967. On the Kolmogorov–Smirnov test for normality with mean and variance unknown. – Am. Stat. Ass. J. 62: 399–402.

Lindström, J., Ranta, E., Kokko, H. et al. 2001. From arctic lemmings to adaptive dynamics: Charles Elton's legacy in population ecology. – Biol. Rev. 76: 129–158.

McKane, A. J. and Newman, T. J. 2005. Predator–prey cycles from resonant amplification of demographic stochasticity. – Phys. Rev. Lett. 94, article no. 218102

May, R. M. 1974. Stability and complexity in model ecosystems. – Princeton Univ. Press.

Moran, P. A. P. 1953. The statistical analysis of the Canadian lynx cycle. – Aust. J. Zool. 1: 163–173.

Nisbet, R. M. and Gurney, W. S. C. 1976. A simple mechanism for population cycles. – Nature 263: 319–320.

Nisbet, R. M. and Gurney, W. S. C. 1982. Modelling fluctuating populations. – Blackburn Press, New Jersey.

Olarrea, J. and de la Rubia, F. J. 1996. Stochastic Hopf bifurcation: the effect of colored noise on the bifurcation interval. – Phys. Rev. E 53: 268–271.

Platt, T. and Denman, K. L. 1975. Spectral analysis in ecology. – Annu. Rev. Ecol. Syst. 6: 189–210.

Renshaw, E. 1991. Modelling biological populations in space and time. – Cambridge Univ. Press.

Rosenzweig, M. L. and MacArthur, R. H. 1963. Graphical representation and stability conditions of predator–prey interactions. – Am. Nat. 97: 209–223.

Sinclair, A. R. E., Gosline, J. M., Holdsworth, G. et al. 1993. Can solar cycles and climate synchronize the snowshoe hare cycle in Canada? Evidence from tree rings and ice cores. – Am. Nat. 141: 173–198.

Trujillo-Ortiz, A. and Hernandez-Walls, R. 2003. DagosP-test: D'Agostino-Pearson's K2 test for assessing normality of data using skewness and kurtosis. A MATLAB file. – [WWW document]. URL: http://www.mathworks.com/matlabcentral/ fileexchange/loadFile.do?objectId = 3954&objectType = FILE.

Turchin, P. and Ellner, S. P. 2000. Living on the edge of chaos: population dynamics of Fennoscandian voles. – Ecology 81: 3099–3116.

van Kampen, N. G. 1981. Stochastic processes in physics and chemistry. – North-Holland, Amsterdam.